CHAPTER 14

BIOGENIC FERRIMAGNETISM: A NEW BIOMAGNETISM

J.L. Kirschvink

Division of Geological and Planetary Sciences
California Institute of Technology
Pasadena, California, U.S.A.

In its simplest form, biomagnetism is usually defined as the study of the magnetic fields originating in living systems, while the term magnetobiology refers to the effects of magnetic fields on organisms. Most biomagnetic research currently in progress today and discussed in other chapters deals with magnetic fields generated either by ionic currents flowing within an organism, those induced para- or diamagnetically by the application of external fields, or those produced by the transient high-field alignment of the magnetic moments of magnetic contaminants. However, there is another proper branch of biomagnetism that warrants discussion here: magnetic moments and fields produced by biochemically precipitated ferrimagnetic minerals. Unlike paramagnetic or diamagnetic substances, a ferrimagnetic particle of the proper size and shape will spontaneously produce a permanent magnetic moment which under normal biological conditions cannot be demagnetized. On a microscopic scale, the magnitude of the local magnetic field adjacent to these particles may be quite large, and the particles will interact strongly with the weak geomagnetic field.

Several topics are relevant in this chapter on biogenic ferrimagnetism. These include the phyletic distribution of known biochemically precipitated iron minerals and their biomineralization processes, the origin of ferro- and ferrimagnetism, and the ferrimagnetic properties of magnetite (Fe_3O_4), which is as yet the only known biogenic ferrimagnetic mineral. Of additional interest is the biological function of these particles in nature. Laboratory techniques for the study of these particles are discussed at length in the last section.

14.1. BIOMINERALIZATION OF MAGNETITE

Living organisms are known to precipitate biochemically over 40 different minerals, many of which have a wide distribution among the phyla (Lowenstam 1981; Lowenstam and Weiner 1982). At present there are ten known iron compounds (Table 14.1.1), of which only one (magnetite) is ferrimagnetic. The general process of mineral formation by organisms appears to span a spectrum between those which are formed with a high level of biochemical control exerted by an "organix-matrix" mediated process, and those which form with less control through a "biologically-induced" process (Lowenstam and Weiner 1982).

Biologically-induced minerals generally have crystal habits that are similar to those seen in their inorganic counterparts, and typically the crystallite size and orientation vary markedly from grain to grain. Although the organisms clearly supply and locally concentrate the chemical components for biomineralization, they exert little control on the crystallization process itself.

In contrast, matrix-mediated minerals are usually grown in a pre-formed organic framework (the matrix) which may exert control over the size, shape, and even crystallographic orientation of the precipitate. As noted by Lowenstam (1981), the precision of this processs is such that many organisms are able to make minerals that cannot otherwise form through inorganic processes elsewhere in the biosphere.

The formation of magnetite is a clear example of a matrix-mediated biochemical process, and this process has been best studied in the chitons, Polyplacophoran molluscs (Towe and Lowenstam 1967; Kirschvink and Lowenstam 1979), and in the magnetotactic bacteria (Frankel et al. 1979; Balkwill et al. 1980; Blakemore et al. 1979; Towe and Moench 1981). Prior to its discovery in chiton teeth (Lowenstam 1962), it was known to form as a high temperature and pressure phase in igneous and metamorphic rock. It is not thermodynamically stable in the oxidizing environment at the earth's surface, and, if left unprotected, fine particles will slowly oxidize to maghemite (γFe_2O_3), hemaetite (αFe_2O_3), or a variety of other iron minerals. The degree of biochemical control in the process of magnetite formation can be seen clearly in the electron micrographs of Figs. 14.1.1 through 14.1.4. A fibrous network or organic matrix material, which appears as the light meshwork in Figs. 14.1.1b and c, surrounds individual magnetite crystals exposed at the chiton tooth's surface. This meshwork is assembled early in the tooth formation process, prior to any biomineralization event. During this pre-mineralization stage, ferric iron accumulates in the superior epithelial cells surrounding the tooth, and after a few days is slowly transported into the organic meshwork and deposited as the mineral ferrihydrite (Towe and Lowenstam 1967; Kirschvink and

Table 14.1.1. The diversity and distribution of iron-bearing biogenic minerals in extant organisms. (From Lowenstam and Weiner 1982, and the Jarosite from Lazaroff et al. 1982)

	Jarosite	Amorph. Fe-Ca Phosphate	Hydrotroilite	Pyrite	Amorphous Ilmenite	Amorphous Ferrihydrite	Ferrihydrite	Lepidocrocite	Goethite	Magnetite	
MONERA	*		*	*		*	*	?		*	Bacteria
PROTOCTISTA										?	Chlorophyta
						*					Foraminifera
FUNGAE							*				Basidiomycota
							*				Deuteromycota
PLANTAE							*				Bryophyta
							*				Tracheophyta
								*			Porifera
											Platyhelminthes
ANIMALIA		*				*	*				Annelida
		*					*	*	*	*	Mollusca
										*	Arthropoda
		*			*						Echinodermata
						*	*		*	*	Chordata

Lowenstam 1979). After the bulk of the iron is in place, the reddish ferrihydrite is rapidly reduced to magnetite, and can be seen as a sharp red/black change between sequential teeth on the radula (tongue plate). Magnetite formation in chitons always proceeds through the reduction of a ferrihydrite precursor, even in the late stages of tooth maturation.

Magnetotactic bacteria also exhibit similar matrix-mediated

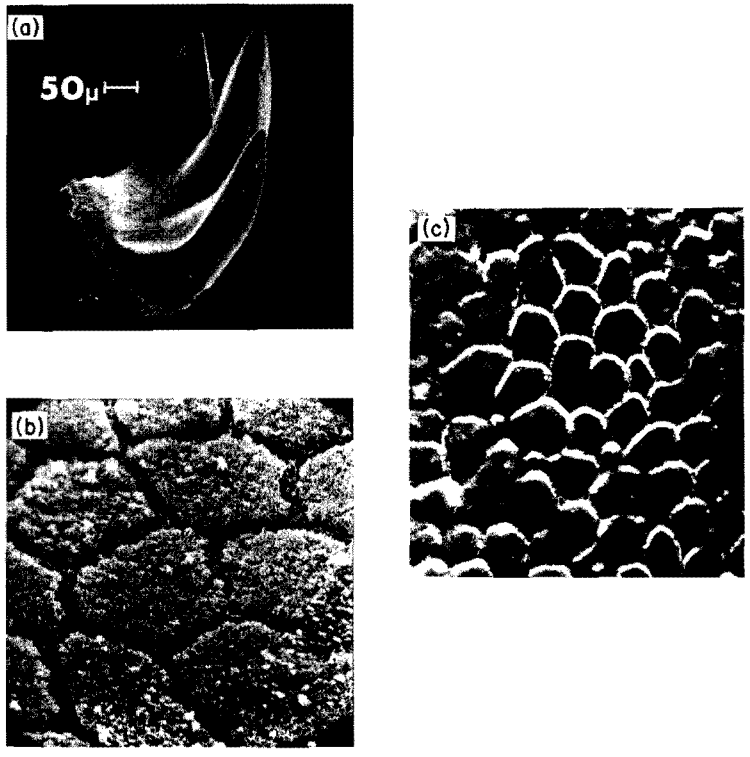

Fig. 14.1.1. (a) A mature magnetite-bearing tooth of the chiton, Poneroplax pateliana, from New South Wales, Australia (scale: 50 μm). (b) The surface of a Chiton tuberculatus tooth, showing the organic matrix superstructure surrounding aggregates of fine-grained magnetite crystals. (c) Surface replica of a C. Stelleri tooth viewed with transmission electron microscopy. The light bands are fibers of the organic matrix surrounding the magnetite crystals. (SCM photo-micrograph (b) is courtesy of H.A. Lowenstam; (c) used with permission of K.M. Towe)

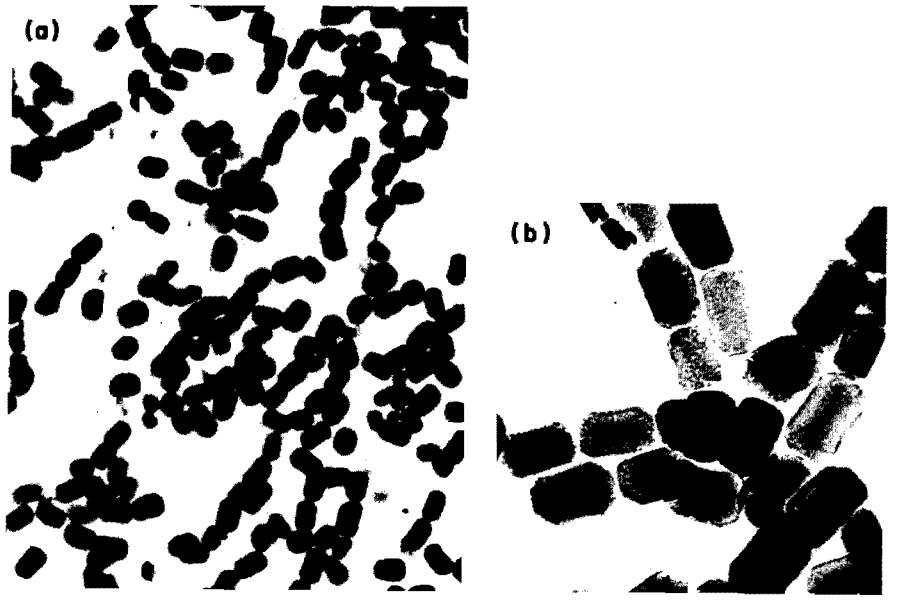

Fig. 14.1.2. Bacterial magnetite crystals (courtesy of K.M. Towe). Small inclusions of organic material may be seen in (b) (Towe and Moench 1981).

control over the magnetite biomineralization process. Balkwill et al. (1980) found that the crystals were formed within an intracellular organelle termed a "magnetosome" which held them together in a linear chain. Mature crystals produced by a bacterial strain are of extremely uniform size and shape. The most common crystal morphologies observed to date are hexagonal parallelipipeds with flat ends shown in Figs. 14.1.2a and b (Towe and Moench 1981), although Blakemore et al. (1980) found a New Zealand bacterium with a novel "teardrop" shape. Evidence for the crystalline nature of these particles is provided by the electron diffraction pattern shown in Fig. 14.1.3. Crystals within the magnetosomes are aligned in a common direction, along what appears to be the diagonal of the cubic habit (the [111] crystalline axis). The [111] axis is also the "easy" direction of magnetization, that is, the energetically preferred direction for alignment of the magnetic moment. Therefore this crystallographic orientation would yield a slightly higher magnetic moment for a given particle volume. Magnetite crystals of inorganic origin usually have an octahedral shape; the hexagonal and teardrop forms are truly novel biogenic forms which are easily distinguished from their inorganic counterparts. The bacteria may also form their magnetite through conversion of a ferrihydrite-like compound (Frankel et al. 1979).

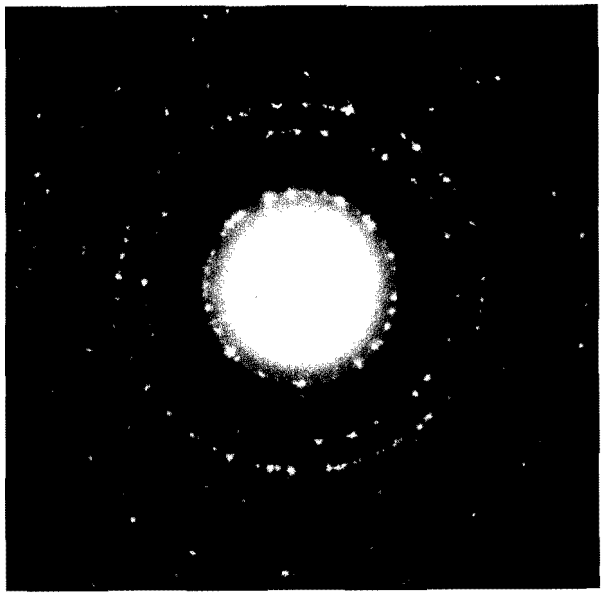

Fig. 14.1.3. Electron diffraction pattern from bacterial magnetites like those of Fig. 14.1.2. The ring spacing and spot patterns are distinctive for magnetite. (Courtesy of K.M. Towe)

As will be discussed in the second half of this chapter, magnetite can also be found and extracted from a variety of higher animals such as oceanic fish and sea turtles. As shown by the scanning electron micrograph in Fig. 14.1.4, this material has distinctly different morphology than magnetite of inorganic origin. Although magnetite is a common industrial pollutant which can often find its way into the food, gut, and intestinal track of higher animals, there is as yet no evidence that particles of it can cross the internal and external barrier of epithelial cells and move into the blood stream to be carried around the body. If this were the case, one would expect to find magnetic particles of external origin randomly scattered throughout the body, and this is not observed in most organisms. The low pH environment of the vertebrate gut will tend to destroy magnetite chemically. Occasional bits of magnetic material are found associated with gills, eye sockets, old wounds, and very often with the skin, but most of this is clearly contamination and not highly reproducible from individual to individual. By comparison, internal tissue such as muscle, nerve, and internal organs are usually quite low in magnetic material.

With the exception of chitons, very little is known about the biomineralization process of magnetite in higher organisms. Al-

though minute amounts of this material can be detected by using the SQUID moment magnetometers described later, the material is small in volume and difficult to locate uniquely using the transmission electron microscope. However, it is clear that the magnetite formed by honey bees and monarch butterflies is of biogenic origin because the stable remanence first develops during metamorphosis (Gould et al. 1978; Gould 1980; Jones and McFadden 1982, and pers. comm. 1982; Kirschvink unpubl.). During this time, nothing enters or leaves the bee pupae or butterfly chrysalids, implying that the magnetic material must form in situ. Similarly, the narrow grain-size distribution measured for pigeon magnetite reported by Walcott et al. (1979) and the consistent localization of magnetite in or near the ethmoid region in the head of many vertebrates (Kirschvink 1982a) and their unique crystal morphologies (Fig. 14.1.4) all argue for a biogenic origin of this material. A further clue is the high purity of this material as shown by electron microscope analysis. Geological magnetites usually have appreciable impurities such as titantium and other trace metals.

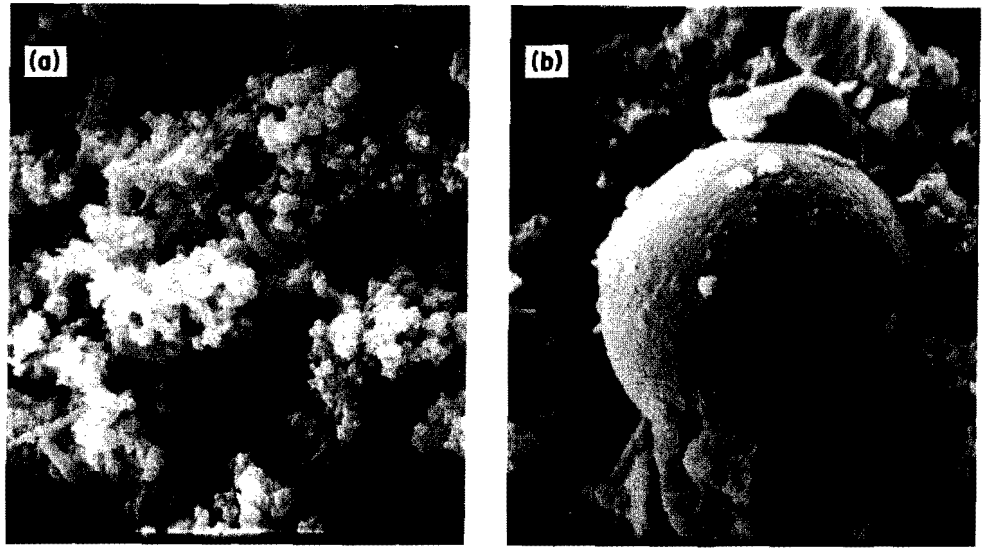

Fig. 14.1.4. (a) SEM micrograph of magnetite extracted from the ethmoid complex of Yellowfin tuna. The typical grain size is on the order of 0.1 μm, although the crystals have clumped together (Courtesy of M.M. Walker). (b) In both the tuna ethmoid tissue and in dura from the green sea turtle (this picture), anomalous spheres of magnetite 5-50 μm in diameter have been found. Their function (if any) is as yet unknown, but in surface detail they do not resemble inorganic magnetites (Courtesy of A. Perry).

In summary, magnetite is one of a variety of iron minerals which are formed under strict biochemical control. As shown in Table 14.1.2, however, it is unique among them in a variety of its biochemical and physical characteristics. It is the ferrimagnetic properties which are of principal interest in biomagnetism and of concern next.

14.2. FERRO- AND FERRIMAGNETISM

Any discussion of biogenic ferrimagnetism must answer the question of why a mineral like magnetite is any different in its magnetic properties than the other biochemically-precipitated iron compounds listed in Table 14.1.1. The answer lies in the crystal structure. At temperatures above the Verwey transition (120 K), magnetite has an overall cubic symmetry in its crystalline array of atoms and is classed as an inverse spinel. Oxygen atoms are in close cubic packing, with Fe^{2+} and Fe^{3+} ions occupying adjacent

Table 14.1.2. Unique biochemical and physical properties of magnetite.

Physical Parameter	Related Value	Comment
Ferrimagnetism	48×10^{5} A/m	Only known ferromagnetic material of biochemical origin
Curie temperature	853 K (580^{o} C)	
Electrical resistivity	5×10^{-5} Ω·m	Lowest electrical resistivity of any known intracellular precipitate (≈6,000 times less than cytoplasm).
Density	5.1×10^{3} kg/m^3 (5.1 g/cm^3)	Most dense intracellular precipitate
Hardness	≈6 on Moh's scale	One of the hardest known bioinorganic minerals; chitons use it in their teeth
Color	Dark blue, almost black	Due to photons absorbed by electrons hopping between Fe^{2+} and Fe^{3+} ions

sites within the lattice, having octahedral and tetrahedral symmetry of the surrounding atoms. As a consequence, the iron atoms in magnetite are held very close together (≈0.6 nm apart) and are separated from each other only by single oxygen atoms. Under these conditions, the unpaired electrons in the iron's partially filled d-orbitals will interact strongly.

In ferromagnetic crystals, these unpaired electron spins are forced into parallel alignments such that their small magnetic spin vectors (each with a magnitude of one Bohr magneton, μ_B) add together linearly. This alignment results from a quantum-mechanical "exchange" associated with overlapping electron states between adjacent iron atoms in the closely-spaced crystal lattice. The total magnetic dipole moment "M_D" for a uniformly magnetized ferromagnetic particle is then simply $M_D = n\mu_B$, where "n" is the number of aligned electron spins present in the whole crystal. A ferromagnetic particle only a few tens of nanometers in size may have millions of these magnetic vectors (several from each iron atom). This parallel alignment of small moments is what distinguishes ferromagnetic material from other magnetic and paramagnetic compounds.

Magnetite has a slightly different variety of ferromagnetism, however, which is called ferrimagnetism. The presence of regularly-spaced oxygen atoms in the lattice and their participation in electron exchange between iron atoms on either side makes the electron spins in alternate crystallographic layers antiparallel to each other. Because the Fe^{2+} and half of the Fe^{3+} ions are distributed in alternate crystallographic layers, the net effect is that moments from the Fe^{3+} ions cancel, and a parallel array of spins from Fe^{2+} ions add to form a ferromagnetic-like moment. A ferrimagnet is a material such as this in which atomic moments point in opposite directions but there remains an imbalance and hence a net magnetic moment. It is worth noting that two other biogenic iron minerals, goethite and jaroite (Table 14.1.1), are antiferromagnetic, which means that the antiparallel moments from opposite layers exactly cancel. A weak remanent moment is sometimes seen in goethite as a result of ordered defects in the crystal lattice, but this effect has not been observed in the goethite-bearing teeth of the archeogastropod, Lottia gigantea (Kirschvink, unpubl.).

14.3. STABILITY AND COERCIVITY OF MAGNETIZATION

This large-scale alignment of electron spins across the volume of a ferro- or ferrimagnetic particle gives rise to a variety of macroscopic physical properties which are of interest to the study of biogenic ferrimagnetism. Of particular importance is the influence of particle size and shape on the directional stability of the spontaneous moment and its microscopic coercivity.

The magnetic stability properties of ferrimagnetic minerals such as magnetite are extremely important to the magnetic tape industry as well as to the geophysicists studying rock and paleomagnetism. The term "stability" as used here simply means the tendency of the magnetic moment vector of a particle to remain fixed relative to the particle's crystal axes. Two factors play a role in this: the total number of aligned electron spins present (e.g. the volume) and the particle's shape. The magnetic dipole moment of a particle has an energy of orientation in an external magnetic flux density B given by $E = -M_D B\cos\theta$, where θ is the angle between the $\mathbf{M}_D$ and $\mathbf{B}$ vectors. This expresses the fact that the orientation of lowest energy is for $\theta = 0$, when $\mathbf{M}_D$ is parallel with $\mathbf{B}$. Note that the moment for a uniformly magnetized particle is simply the volume times the saturation magnetization, the latter being 4.8×10^5 A/m for magnetite. For extremely small particles in the ≈50 μT geomagnetic field, this implies that the "energy product" $M_D B$ per crystal may be less than the average thermal energy ($\approx k_B T$ or 4.2×10^{-21} joules at room temperature). Random realignment of the electron spins because of thermal agitation will then cause the direction of the moment vector to wander constantly relative to the crystal axes. This type of magnetic instability is said to be superparamagnetic, because the application of even a relatively weak magnetic field causes a substantial rotation of the particle's moment toward the field direction, and hence the particle exhibits an extraordinarily large paramagnetic susceptibility. Superparamagnetism is characteristic of particles with sizes and shapes that fall in the lower region of Fig. 14.3.1.

On the other hand, the magnetic moment of much larger particles would set up a substantial magnetic field in the surrounding space, which is energetically unfavorable, and the parallel alignment of electron spins will collapse into two or more smaller regions ("domains") with moments pointing in different directions so as to reduce the external field energy. The simplest configuration has two oppositely directed domains whose moments cancel. Then the net moment of the particle arises solely from the electron spins in the "wall" between the two domains, where the magnetization rotates in spiral fashion by 180° from one domain to the other. Such particles are said to be "pseudo-single domain" since only one region - the wall - contributes to the particle's moment. The net magnetic moment of a two-domain particle, or for larger particles a multi-domain configuration, is much reduced from that of the totally aligned configuration. Such particles are represented in the upper area of Fig. 14.3.1.

Particles that lie intermediate in size between the superparamagnets and multi-domain configuration have a uniform magnetization and are stably magnetized, and hence they are described as having a single-domain. Highly elongated particles tend to favor the single-domain state, an effect which is due to their shape an-

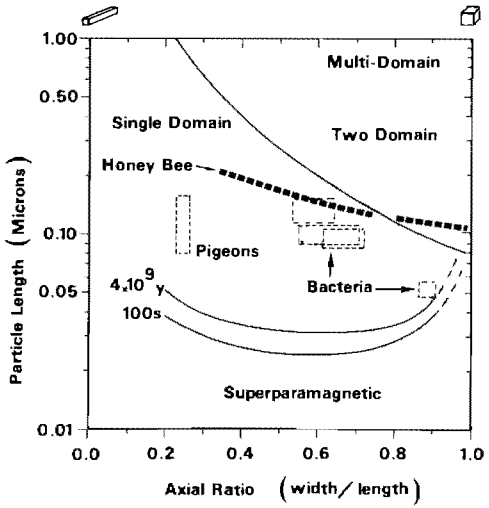

Fig. 14.3.1. Size-shape relationships and magnetic properties of magnetite crystals (after Butler and Banerjee 1975). Each point on this diagram represents a rectangular magnetite crystal of specified size and shape. The two lines at the bottom show all particles with time constants between 100 seconds and 4×10^9 years. Numerous bacterial and pigeon magnetite crystals that have been measured by electron microscopy all plot in the single-domain field as shown. The dashed line corresponds to those crystals which have the volume of magnetite estimated for the honey bee compass receptor from their horizontal dance (Kirschvink 1981).

isotropy. Particles of this size and shape will always be magnetized fully to the saturation value and cannot be demagnetized under biological conditions. It is not necessary to magnetize these particles as their moments form spontaneously. These are the particles that are clearly involved in bacterial magnetotaxis, the basis for the magnetic tape industry, and most likely relied on for the magnetic field sensitivity in higher organisms.

The boundary in Fig. 14.3.1 between the superparamagnetic and single-domain particles is not sharply defined, but is based on the time scale that describes the rotation of the moment vector relative to the particle. A change in size of a few nanometers, however, is enough to change this time from less than 100 seconds to more than 4 billion years. Paleomagnetists have devised a variety of indirect magnetic experiments discussed at length in the latter half of this chapter which can distinguish these various forms of stability from each other without needing to isolate and purify the magnetic minerals.

One measure of the magnetic stability of a ferro- or ferrimagnetic particle is termed its "coercive field." In an elongated single-domain particle, the shape anisotropy constrains the magnetic moment to lie either parallel or anti-parallel to the particle length, unless forced out of alignment by a strong magnetic field. The coercive field is the field intensity at which the moment is first flipped from one stable orientation to the other. Several of the techniques discussed in the latter portion of this chapter depend upon this property.

14.4. EVOLUTION AND FUNCTION OF BIOGENIC MAGNETITE

Very little is known at present about the evolutionary history of the biochemical pathway(s) for magnetite biosynthesis. Part of the problem is the lack of a direct fossil record. The small grain size of bacterial crystals gives them a large ratio of surface to volume, which speeds their conversion to other minerals after the bacteria die (Demitrack 1981), although there is some paleomagnetic evidence for bacterial magnetite in Miocene marine clays from Crete (Kirschvink 1982b). Chitons first appear and diversify in the fossil record during late Cambrian and early Ordovician time ($\approx 510 \times 10^6$ years ago), so it seems likely that the biochemical pathway in molluscs evolved sometime prior to this during the Precambrian period. The presence of intracellular chains of magnetite crystals in modern anaerobic or microaerophillic bacteria suggests the possibility that it may originally have served as an iron storage material in the chemically reducing environment of the early Precambrian. The global switch from a reducing to oxidizing environment would then have provided strong evolutionary pressure favoring bacteria that exploit any advantage of having internal magnetic particles. Two such advantages might result from the orienting effect of the geomagnetic field: it could serve to guide bacteria away from oxygen-rich surface waters while they swim, and it could prevent them from moving in a "random walk," which would make progress less efficient. An orienting effect due to magnetic torque is called magnetotaxis, and this has been observed in several types of marine and freshwater bacteria as well as in one green algae (Chlammydomonas sp.) by Lins de Barros et al. (1981). Fossil crystals of bacterial magnetite ought to be easily recognized in the fossil record by their unique hexagonal shape, but the systematic search for them is just beginning.

The function of biogenic magnetite is only clearly known for the chitons, magnetotactic bacteria, and perhaps the magnetotactic algae. Chitons harden their major lateral teeth with magnetite so they can be used for scaping algae off of rocks. Magnetosomes within the bacteria contain enough single-domain magnetite to passively align their cells in the geomagnetic field, even after they die (Frankel and Blakemore 1980). When alive, they generally swim

northwards (and downward) in the Northern hemisphere, southwards (and downward) in the Southern hemisphere, and in both Northern and Southern directions on the geomagnetic equator (Blakemore 1975; Kirschvink 1980; Blakemore et al. 1980; Frankel et al. 1981). It has been suggested that the downward orientation is the most significant one in that it directs the bacteria towards anoxic muds and nutrients at the mud/water interface. That magnetotaxis is indeed the function of bacterial magnetite is supported by the observation that all known bacterial crystals measured to date with transmission electron microscopy are represented only within the single-domain region shown in Fig. 14.3.1. This is not true for all crystals measured in chiton teeth which are not used for magnetic orientation (Kirschvink and Lowenstam 1979; Towe and Lowenstam 1967). The single-domain configuration represents the greatest economy in terms of a particles net magnetic moment per volume of material. A mutant bacterial strain which happened to form superparamagnetic or multi-domain crystals would quickly be eliminated by natural selection.

In higher organisms the most probable use of biogenic magnetite is for magnetoreception, either as a "compass" to aid navigation or perhaps as a receiver of time or "map" information (Kirschvink and Gould 1981; Kirschvink 1982a). However, the list of unique biochemical and physical properties for magnetite in Table 14.1.2 suggests many other possibilities. Support for the magnetoreception hypothesis comes from several sources, including the discovery of biogenic magnetite in virtually every known magnetically sensitive organism, including elasmobranch fish (sharks and rays) which are known to have both electric and magnetic senses. As will be discussed, additional support comes from the observation that the horizontal magnetic dance of the honeybee can be explained by a mechanism based on a single-domain ferromagnetic compass (Kirschvink 1981), and that most suggested alternative strategies for magnetoreception (such as electroreception) do not work well in small terrestrial or freshwater animals (Jungerman and Rosenblum 1980; Tesch 1980). Note that a magnetic compass is as viable an hypothesis to account for the elasmobranch magnetic sense as is the use of their ultra-sensitive electroreceptors. Behavioral experiments have not yet resolved this question.

Although the study of the magnetically influenced behavior of animals is more properly called magnetobiology than biomagnetism, it is worth briefly discussing it here. More extensive reviews of this literature have been presented by Adey and Bawin (1974), Gould (1980), Ossenkopp and Barbeito (1978), and Kirschvink (1982a). The evidence suggests that animals have two basic types of magnetosensory systems, one of which is used for compass orientation and another for deriving map or time information from the geomagnetic field. For brevity, only the compass sense in homing pigeons and honey bees will be considered here.

Keeton (1971) and Walcott and Green (1974) were the first to demonstrate reliably that homing pigeons possess a magnetic compass sense, although Yeagley (1947) had claimed this much earlier. Trained birds are normally able to orient themselves quickly and depart in the homeward direction when released at an unfamiliar site on a sunny day (Fig. 14.4.1, top row). However, paired coils wrapped around their heads or small magnets attached to their backs predictably disorient their departure bearings on cloudy days (Fig. 14.4.1, bottom row). These data imply that the magnetic compass is only used when the primary sun compass is not available. Similar experiments with migratory European robins (Wiltschko and Wiltschko 1972) as well as pigeons imply that these animals sense the dip angle of the field (i.e. the maximum angle of the field relative to the horizontal) and are not able to distinguish magnetic north from south.

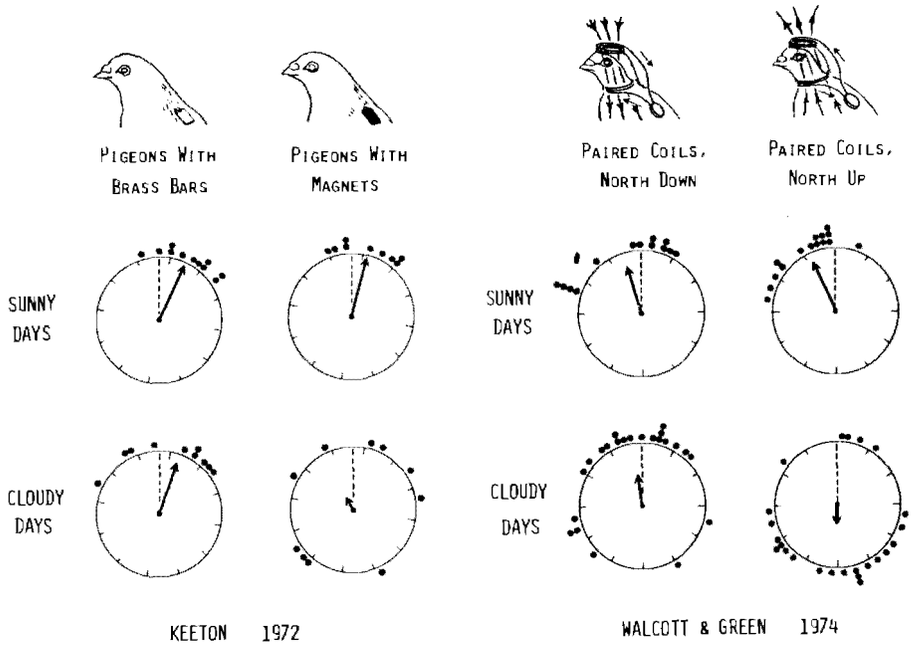

Fig. 14.4.1. Influence of a magnetic field on the bearings of trained homing pigeons as they leave the sight of the observer following release. On sunny days (top row of circular diagrams), most birds are able to depart in the general direction of home (dashed lines) with reasonable accuracy (indicated by the length of the mean departure arrows). However, on cloudy days when the sun is not visible (bottom row of diagrams), a small magnet attached to their backs disorients many of the birds, whereas a brass bar of similar size and weight has no effect. Also on cloudy days, paired coils which reverse the dip direction of the field around the bird's head (North up) causes them to fly in the wrong direction, whereas identical coils producing a downward field (like that in the Northern Hemisphere) have little effect. Data are from Keeton (1971) and Walcott and Green (1974).

A variety of similar magnetic compass effects have been reported in honey bees (Martin and Lindauer 1977; Gould 1980). The clearest response is found in their horizontal waggle dance - if a beehive is tilted on its side such that the normally vertical sheets of honey comb are placed horizontally, the bees can be deprived of their usual gravity reference cue in their dance language. After this is done, and in the absence of other orientation cues such as polarized light, dances are initially disoriented. Two or three weeks later, however, if a horizontal magnetic field up to 500 μT is applied the dance of the bees is preferentially aligned along 8 points of the magnetic compass (Fig. 14.4.2). Stronger background fields enhance this orientation, while

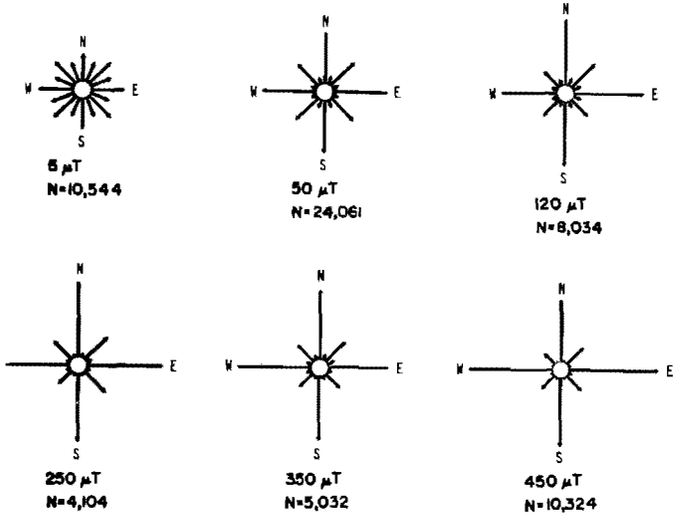

Fig. 14.4.2. Horizontal magnetic dance of the honey bee (data from Martin and Lindauer 1977). The four cardinal directions (N, E, S and W) shown on the rose diagram for each dance are measured with respect to the local magnetic field in the hive. The N value tells the number of individual dances measured for each diagram. In weak background fields the orientation is poor, whereas it reaches an apparent maximum in fields stronger than about 200 μT.

weak fields reduce it. The quantitative agreement between this alignment response and that expected statistically for a magnetic dipole (the "Langevin function," discussed by Kittel, 1976) suggests the presence of a "magnetic compass" (Kirschvink 1981). Other compass responses have been reported in salmon (Quinn 1980), elasmobranchs (Kalmijn 1974), cave salamanders (Phillips and Adler 1978), eels (Tesch 1980), and wood mice (Mather and Baker 1981).

In concluding this first section, it is worth noting some of the results and predictions about magnetoreception which the magnetic compass hypothesis has to offer. Yorke (1979) has shown that only a few hundred, freely-rotating, single-domain crystals would be more than enough to provide an animal with an extremely accurate magnetic compass sense. The moment of each crystal experiences a torque that tends to rotate it into alignment with the field, but thermal agitatation tends to disrupt any such alignment. The average alignment that results is given by the Langevin function mentioned above, whose value depends on the ratio of magnetic to thermal energies ($M_D B/k_B T$). Thus the organism needs to monitor the orientation of only a few crystals to gain a reasonably accurate compass sense, and the entire compass system might fit into a volume a few micrometers in linear dimension.

A consequence of this is that the SQUID moment magnetometers discussed in the next section are not yet sensitive enough to detect this hypothetical structure. The situation is different, however, for a magnetic system which extracts time or map information from weak fluctuations in background geomagnetic intensity. Two independent analyses (Yorke 1981; Kirschvink and Gould 1981) both suggest that large numbers ($10^6 - 10^7$) of discrete magnetite-bearing sensory organelles are required for this system to function. As a consequence, this structure would be well within the resolution of presently available SQUID moment magnetometers. The magnetic compass hypothesis also predicts, from the standpoint of efficiency and natural selection, that magnetite crystals actually involved in magnetoreception should be of single domain size, as indeed are the bacterial crystals. This appears to be the case as well for the pigeon magnetite as reported by Walcott et al. (1979). Extensive use of the comparative SQUID magnetometry techniques discussed next on 10 species of pelagic fish, dolphins, sea turtles, rodents, and primates has localized a candidate for the magnetic sense organ in or near the region of the ethmoid bones in the vertebrate skull (Walker et al. 1981, and in prep.; Baker et al. 1982; Mather et al. 1982). Whether or not this is indeed a vertebrate sensory organ awaits the outcome of numerous magnetometric, behavioral and neuroanatomical studies.

14.5. LABORATORY ENVIRONMENT AND TECHNIQUES

Many of the instruments and techniques currently used in the study of biogenic ferrimagnetism were originally developed for the analysis of magnetism in rocks, and are discussed in depth by McElhinny (1973). Although rocks and living organisms are clearly different materials, the presence of magnetite in animals implies that similar laboratory techniques ought to be of use in biomagnetic studies. This section is concerned with how these paleomagnetic techniques can be applied to biomagnetism and the variations to them which are sometimes necessary.

14.5.1. SQUID Magnetometry

The key to finding small concentrations of permanently magnetic material in animal tissue is to use the SQUID moment magnetometers which were commercially developed for the study of fossil magnetism in rocks ("paleomagnetics"). These instruments are designed to measure the direction and magnitude of the remanent magnetic moment possessed by samples at room temperature, and their applications to paleomagnetics have been reviewed by Goree and Fuller (1976). Moment magnetometers differ substantially from the other SQUID systems discussed elsewhere in this volume which are designed to measure external magnetic fields or field gradients. The superconducting components include the rf- or dc-SQUIDS discussed in Chapter 4 and flux transformers discussed in Chapter 5. The difference in a moment magnetometer is that the detection coil that serves as the primary of the flux transformer is wound as a Helmholtz pair, inside of which is a room-temperature chamber for the sample. An access port allows the insertion of samples from above or below, while maintaining them at room temperature (Fig. 14.5.1). The insertion of a sample which possesses a weak remanent magnetic moment causes a persistent current to flow around the flux transformer, and as this current flows through the input coil serving as the secondary of the transformer a magnetic field is imposed on the SQUID. The magnitude of this current is proportional to the component of the sample's moment vector lying parallel to the axis of the Helmholtz coils.

This coil geometry minimizes the effect of an inhomogeneous distribution of magnetic material within a sample and makes the instrument less sensitive to its position. Typical instruments use two or three mutually-orthogonal Helmholtz coils, each connected to a separate SQUID system to measure simultaneously two or three components of the moment of a sample. Walton (1977), however, describes a less expensive system using only one SQUID with the vertical and horizontal Helmholtz coils connected together in series.

Four measurements separated by sample rotations of 90° around the vertical provide averaged estimates for all three components of the moment. In all systems, a superconducting lead shield surrounds the

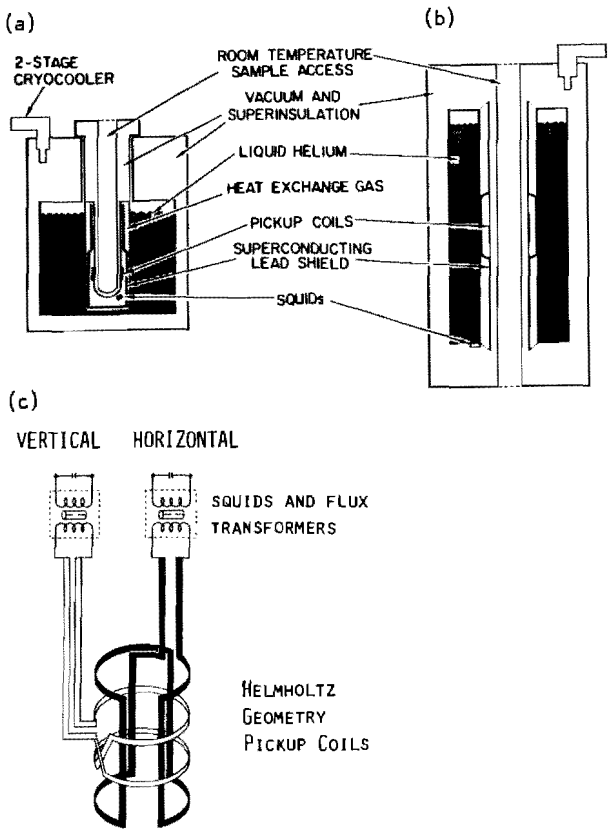

Fig. 14.5.1. SQUID moment magnetometers. (a) Typical geometry commercially produced by United Scientific, Inc., which has a removable cold probe and a vertical sample access port (Goree and Fuller 1976). There are two separate high-vacuum regions as well as a region for helium gas, which cools the superconducting magnetic shield. (b) A newer design made by 2G Enterprises, Inc., (Goree and Goodman, pers. comm.) eliminates the gas region, has only one high-vacuum region, and has the sample access port passing completely through the instrument. The liquid helium dewar is all aluminum, which unlike fiberglass prevents helium from diffusing through walls maintained at room temperature. (c) Arrangement of the orthogonal Helmholtz-style pickup coils (adapted from Goree and Fuller 1976).

superconducting components and attenuates external field fluctuations by factors greater than 10^6. If the system is initially cooled to liquid helium temperature in a low-field environment, the shield will preserve and stably maintain the this field within the measurement area. Fields less than 1 nT are easily trapped in the commercially available systems; this level is low enough to allow the ferromagnetic remanence to dominate over paramagnetic or diamagnetic moments in most biological samples during the measurement procedure.

The sensitivity of commercially-available SQUID moment magnetometers largely depends on the size of the room temperature sample chamber. A large volume reduces the effectiveness of coupling between the moment and detection coil, and the correspondingly larger Helmholtz coils detect more Nyquist noise from conducting components of the dewar, such as the superinsulation in the vacuum space. Goree and Fuller (1976) describe an access system of 3 mm diameter having a peak-to-peak noise level, expressed as the equivalent magnetic moment of the sample, of 0.2 $pA \cdot m^2$. Instruments with the more typical 3.8 and 6 cm sample access ports have noise levels in the range of 1 to 10 $pA \cdot m^2$. By comparison a typical 0.1 μm crystal of single-domain magnetite has a moment of about 0.5 $fA \cdot m^2$, so only about 10^3 to 10^4 such crystals need to be aligned in a sample before their net moment can be measured. A 9 mm^3 vertebrate tissue sample has about 3×10^7 cells, so this resolution implies that the presence of about one 0.1 μm crystal for every 30,000 cells can be detected. Instruments with larger sample-access ports can, of course, accommodate greater numbers of cells, but their slightly lower sensitivity yields a roughly comparable resolution per cell.

The last item of concern with regard to the routine laboratory operation of SQUID moment magnetometers is the rate at which they consume liquid helium and the frequency with which their helium dewars need to be refilled. Spot-shortages in the supply of helium have already been felt in the United States and will most likely continue, so it is desirable to have instruments which are as efficient as possible. Goree and Fuller (1976) note that the commercially available 3.8 cm vertical access instruments will boil off about 4 liters per day, which means that the typical 30 liter dewar needs to be filled once a week. A Stirling cycle cryocooler can cut the helium loss to less than one liter per day, which would allow one month of continuous operation. A recent design (Fig. 14.5.1b) which uses a 100 liter cryo-cooled dewar is expected to extend this maintainance-free operating time to longer than 6 months. Both instuments are described in Fig. 14.5.1.

14.5.2. Soft-Iron Magnetic Shielding

Many methods are employed at present for producing the low

background fields necessary to operate SQUID moment magnetometers (see Chapter 16). Large Helmholtz coils with feedback loops or nested high-permeability shields like Mu-metal and molypermalloy can reduce the ≈50 μT geomagnetic field to less than 1 nT in the region of the superconducting lead shield. Once the lead is superconducting it traps the low field and allows the SQUID magnetometer to operate even if the whole instrument is moved out of the low field environment. Unfortunately, many of the techniques used to analyze the magnetic properties of a sample also require low fields (<100 nT) and will not work well if a sample is repeatedly exposed to the geomagnetic field between magnetic measurements. An ideal laboratory environment would therefore have the magnetometer and work area in one large low-field space. Shielded areas of this size are not easily or inexpensively built with either Mu-metal or electrical coil systems.

A comparatively cheap, easily constructed solution to this problem has recently been reported by Scott and Frohlich (1980). They use 0.5 mm thick rectangular sheets of magnetically-soft transformer steel which are anhysteretically magnetized parallel to their long dimension. Although these sheets are multi-domain aggregates, some of the domain walls move easily in response to ambiant field variations, while others remain strongly pinned after they are magnetized. Scott and Frohlich place these sheets in two layers separated by about 30 cm to cover the floor, walls, and ceiling of the laboratory area, taking care that each sheet is aligned with its magnetization in the northward direction. When arranged in this fashion, the moments from all of the sheets add together and produce a uniform field within the enclosure that is antiparallel to that of the earth. By adjusting the number and position of the steel sheets within each layer the residual field within the enclosure can be reduced to a few tens to hundreds of nanotesla. Domains which are strongly pinned will maintain the low field environment almost indefinitely, while the rest will slowly counteract diurnal and other laboratory-induced variations. Relatively cheap thin-walled Mu-metal cans or foil can then be used to reduce the field further wherever required.

We recently used about 2,000 kg of steel (about $6,000 worth) in the construction of a shielded lab with inside dimensions (length, width, and height) of 4.1×2.9×2.8 meters respectively. The outer layer of shielding is a rectangular box measuring 4.8×3.6×3.5 meters, aligned in the North/South direction with a northeasterly "snail-shell" entrance. Each layer of steel is sandwiched between sheets of plywood and epoxy-coated plaster board to prevent the steel from warping, and the assembly is held together with aluminum nails and brass screws. Immediately after construction we demagnetized the steel with a strong 60 Hz alternating field produced by an elongated coil, and the field inside the room dropped to less than 50 nT over most of the volume. After 3 months of heavy use this

rose irregularly to an average of 200 nT, but the initial low field was recovered by another demagnetizing. The particle-free environment described next is housed within this low-field enclosure.

14.5.3. Laboratory Environment

The extreme sensitivity of the SQUID moment magnetometer demands that great care be taken to prevent accidental contamination of biological samples during the measurement procedures. A wide variety of ferromagnetic materials are found in the normal laboratory environment, and small dust-sized particles from them can easily be blown around in the air and may lie in wait on exposed surfaces after they settle. Cast-iron pipes in particular have a tendency to rust, and biological samples washed in water from a building with old plumbing can suddenly gain spurious moments. A 10 μm dust-sized magnetite particle, for example, has a saturation magnetization of about 500 $pA \cdot m^2$, well within the sensitivity range of SQUID moment-magnetometers. Great care must be taken for these reasons to prevent sample contamination during the dissection and measuring process. Two simple methods for reducing the contamination problem need to be discussed next: a clean-lab environment and non-contaminating methods for dissection and sample preparation.

Several problems immediately surface when one attempts to work with a biological sample in a paleomagnetic laboratory. Rock samples tend to leave fine particles behind them and are therefore a major source of ferromagnetic contamination, along with airborne industrial pollution. This problem was temporarily solved by placing thin-walled polyethylene sheets around the SQUID magnetometers and dissecting area, followed by thorough cleaning with glass-distilled water. After a few days, however, the gradual dust accumulation from the air would reach unacceptable levels and the entire work area would need to be cleaned again. The basic problem is that paleomagnetic laboratories are not designed for clean-lab work; the full sensitivity range of SQUID magnetometers is rarely needed for geological studies (measurement speed is more important).

One approach to solving this problem of airborne contamination that we have taken in Pasadena is to constantly inject clean air into the low-field laboratory described above, thereby keeping dust out with positive pressure. The air is passed through a series of paper, fiberglass, and carbon filters which remove 99.9% of all particles above 1 μm size, and 95% in the range from 0.1 to 1 μm. This removes most of the pseudo-single domain and multidomain contamination problem. To further trap ferromagnetic particles of smaller size, the air is also passed through a magnetic "filter" composed of several CoSm magnets surrounded by stainless steelwool ribbon. The high permeability of the steel in a strong magnetic field produces very high gradients along the ribbon edges, which in

turn trap the remaining magnetic particles as they pass. A final fiberglass filter prevents stray bits of steel wool from entering the lab area. At present the main source of contamination appears to be the dust and lint brought in on the clothing and in the hair of people using the lab. Hopefully, this source will be eliminated by wearing lint-free garments and by using a deionized water shower.

14.5.4. Non-Magnetic Dissection Tools

The first problem faced in any attempt to search for magnetic particles in animal tissue is to remove the samples of interest without contaminating them. Several non-magnetic dissection and sample manipulation procedures have proven to be extremely useful for this and are worth briefly describing here. It was noted earlier that typical metal dissection tools such as scalpels, steel pins, scissors, and tweezers can leave trails of highly magnetic particles behind them. More subtle is the observation that even non-ferrous metals like copper and aluminum often contain significant numbers of small ferromagnetic inclusions which make them unsuitable for use as dissection tools or sample holders. Wood, plastic and glass seem to be the three non-magnetic materials best suited for this work, although all can gain measureable moments when exposed to a strong magnetic field. Disposable wooden chopsticks are by far the best tools for handling samples during the cleaning, freezing and measuring procedures. Plastic picnic knives are good for removing large blocks of tissue but not for precisely excising small structures. More precision can be gained by using knives made from freshly-broken glass sheets, similar to those commonly used in the preparation of ultra-thin sections for electron microscopy. Glass knives are fragile, however, and do not work well when cutting through thick pieces of bone such as tuna fish, monkey, or dolphin skulls. For this job, wedges made of oak or a similar hardwood are needed and can be driven in with a rubber mallet. The ideal tool for cutting through thick skull bone, however, would be a diamond-impregnated plastic or ceramic saw blade. This might eliminate many of the metal blade-induced contamination problems noticed in primates and cetaceans. Ultrasonic cleaning either in glass-distilled water or 6N HCl of everything which comes in contact with a sample greatly helps to reduce the contamination problem.

In summary, it is still difficult to conduct precise dissections on small organisms using non-magnetic techniques (see Walcott 1980). However, the methods described here work well on a variety of larger organisms.

14.5.5. Sample Preparation

After a tissue sample of interest has been removed with non-magnetic tools and cleaned in a glass-distilled water, the magnetic particles within it must be immobilized and remagnetized prior to measurement on the SQUID system. This is not normally done for rock samples because the fossil magnetization is usually of greater interest. If small magnetic particles in a tissue sample are suspended in a viscous medium, Brownian motion will tend to quickly disrupt any alignment between moments of the particles. This will cause a decay in the net remanent moment in a room-temperature sample, an effect which is quite commonly observed. Freezing the tissue with liquid nitrogen quickly solidifies a sample and prevents this decrease. Because the thermal energy is reduced, this procedure has the added advantage of reducing the particle size determining the boundary between single-domain and superparamagnetic behavior. For magnetite particles this becomes about 20 nm. Monitoring the net remanent moment as the sample is allowed to warm to room temperature can then supply information about the superparamagnetic particle size distribution (discussed below). Extremely small samples or cell suspensions can likewise be frozen into an ice-cube made of water (distilled in a glass system!) in a flexible plastic tray. Ice-cubes made of distilled water also serve as good control samples for monitoring the level of laboratory air and surface contamination.

Simply freezing a sample, however, is not sufficient preparation for the SQUID magnetometry. At this stage the moments from the individual magnetic particles are still randomly aligned and their vector sum is near zero. In the low field of the SQUID magnetometer, the moment of a single-domain magnetite particle will lie parallel to the long axis, but the direction of its North-South orientation relative to this axis is arbitrary. It is necessary to realign the moments such that their north-seeking ends all have a positive component along the direction of measurement. This can be done by application of a strong magnetic field before the sample is lowered into the moment magnetometer. In this manner the moments from all the particles will add vectorally together and produce a stable, measureable moment, termed by paleomagnetists a saturation "isothermal remanent magnetization" (sIRM). If the orientations of the particle moments are randomly distributed within the hemisphere centered on the direction of the applied field, and if the particles are all single-domain, the observed net remanent moment will equal exactly half of the maximum value obtained when the particles are perfectly aligned (Wohlfarth 1958). The sIRM therefore provides an estimate of the total amount of magnetic material present, a quantity which is of biomagnetic interest.

Highly elongated magnetite crystals have a maximum theoretical coercive field of about 0.3 T, with typical values for biogenic magnetite lying in the range below 0.1 T (Kirschvink and Lowenstam 1979; Kalmijn and Blakemore 1978; Denham et al. 1980; Cisowski 1981). When producing the sIRM in a sample it is desirable to ex-

pose it to a strong uniform field well in excess of this level. We originally tried to align these moments by briefly exposing our samples to a small CoSm magnet which had strong surface fields in excess of 0.3 T. This is not satisfactory, however, because it is difficult to magnetize a large sample uniformly due to the rapid decrease in field strength with distance from the magnet varying as the inverse cube of the distance. An inhomogeneously magnetized sample will yield an underestimate of the amount of magnetic material present and makes it possible to miss important ferrimagnetic structures present in large samples. For similar studies, paleomagnetists normally use large electromagnets to remagnetize their samples in a uniform, controlled fashion. Neither CoSm nor electromagnets are desirable things to have in a magnetically-shielded clean lab, however. Accidentally touching a biological sample to the magnet surface can cause highly magnetic particles to stick and may suddenly produce sample moments from contaminants which are too large to measure on the SQUID system.

A simple solution to this problem is to magnetize the samples with an impulse produced by discharging a bank of capacitors through an aircore solenoid, as shown schematically in Fig. 14.5.2. The circuit is an LC oscillator which is modified to produce only one high-current discharge through the coil. A bank of electrolytic storage capacitors is first charged to a specified voltage with the trigger of the silicon-controlled rectifier (SCR) held off. The SCR is fired by a 5 V trigger while the frozen sample is held in position within the coil, and the circuit temporarily acts like an LC oscillator. Energy stored within the capacitors is transfered to the magnetic field of the solenoid in one-quarter of the resonance period, after which it is dissipated through the large diode. As a result the field within the solenoid remains in the same direction as it builds up to a maximum and then decreases, and will not damage the electrolytic capacitors by trying to charge them backwards.

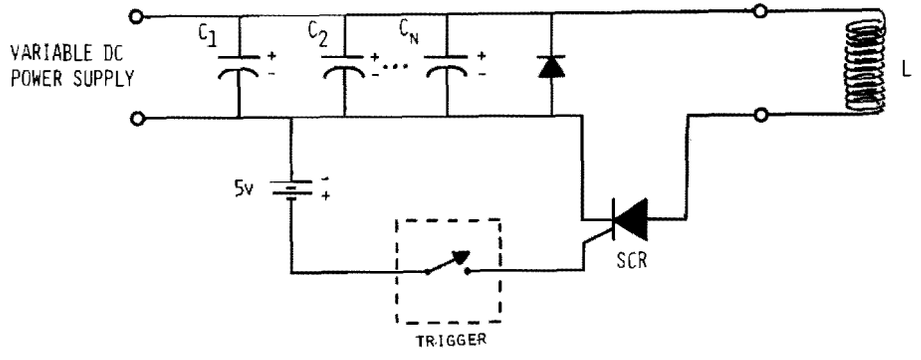

Fig. 14.5.2. Schematic circuit diagram for an impulse magnetizer.

The peak current I_{max} in the solenoid, ignoring resistive loss, is given by $V_o(C/L)^{1/2}$, where V_o is the voltage at discharge, C is the total capacitance, and L is the inductance of the solenoid. The solenoid in use at Caltech consists of 150 turns of 1.6 mm diameter copper wire wrapped in 4 layers on a 13 cm diameter plastic tube, giving an inductance of about 1 mH. With a 6,000 μF capacitance, a 350 V discharge yields a theoretical peak current of 845 A, and a corresponding theoretical peak field of 1.76 T ($B_{max} = 4\pi \times 10^{-7} N I_{max}$, where N is the number of turns per meter). The unit was calibrated by integrating the voltage induced in a small coil during a discharge, showing that about 50% is lost through coil resistance. The overall system is quite linear, with about 2.4 mT per volt of discharge and a measured discharge time of 4 ms. At least 10 volts must be present, however, to switch the SCR properly. Note that a relay should disconnect the charging circuit from the capacitors before the SCR is triggered. Furth and Waniek (1956) describe similar circuits using ignitron tubes rather than SCRs. A system of this sort can generate homogeneous peak fields of several tesla within the coil for discharge times on the order of a few milliseconds; whereas only a few nanoseconds are necessary to magnetize a sample.

14.5.6. Sample Measurements

SQUID moment magnetometers have a room temperature access port into which the samples are inserted; this means that something must hold them in position. In view of the widespread presence of fine-grained ferromagnetic particles in many otherwise "non-magnetic" materials noted above, it is clear that great care must be taken in the construction and use of sample holders. Paleomagnetists generally use mylar, glass, or polyethylene plastic tubes for this, along with small bits of clear plastic tape for holding rock samples in place. These devices also work well for biomagnetic samples, although they may require extensive ultrasonic cleaning with 6N HCl to dissolve surface ferromagnetic particles. A major drawback, however, is that they will pick up a measurable magnetic remanence if exposed to a strong field from either a magnet or an impusle magnetizer. Samples must therefore be magnetized separately from these holders and then loaded for measurement. Frequent checks also need to be made on the empty holders to ensure that they do not become contaminated during use.

It is worth noting here that white cotton thread can sometimes be used as a sample holder in biomagnetic studies without many of the noise problems which plague the more massive holders. A cold sample can be frozen onto one end of the thread and lowered vertically into the sense region of the magnetometer for measurement. If thoroughly cleaned, some cotton and polyester threads do not show any measureable magnetic remanence by themselves and may remain safely attached to the sample. Because the string is free to spin

about the vertical direction, only this component of the moment vector can be measured. This is not a problem, however, because the sample can be magnetized precisely along this axis by suspending it in the vertically-aligned solenoid of the impulse magnetizer. The vertical axis of the SQUID magnetometer will then register the total moment of the sample. Use of this thread greatly simplifies the iterative techniques for finding the spectrum of coercive fields of the particles as described next.

14.5.7. Indirect Methods for Characterizing Magnetic Particles

Any non-destructive technique which might yield information about the size, shape, or composition of the magnetic particles present in a tissue sample is of value in the study of biogenic ferrimagnetism. During the last 25 years, paleomagnetists have developed an impressive array of such techniques for characterizing the magnetic minerals in rocks. The most important and least destructive of these involve the microscopic coercivities, or coercive fields, of the magnetite crystals. The coercive field of a magnetite particle is only a function of its size, shape, and domain state, and is therefore a characteristic property of it. Although individual single-domain crystals cannot as of yet be measured on the SQUID moment magnetometers, the combined moment from large numbers of them can be. The distribution of coercive fields, or "coercivity spectrum," is therefore characteristic of the magnetic particle population and should not change unless drastic chemical effects dissolve or alter the crystals. For single-domain particles, the coercive field increases with particle size and elongation as shown in Fig. 14.5.3 (after McElhinny 1973). Large, multi-domain crystals in general have low coercive fields (<10 mT) due to the easy realignment of domain walls. Two techniques exist for measuring the coercivity spectrum: progressive alternating field (Af) demagnetization and IRM acquisition.

The determination of a coercivity spectra by progressive demagnetization begins by giving the sample a saturation IRM with an impulse magnetizer or magnet as described earlier. After this, all of the particle moments are aligned with the N-seeking directions in the hemisphere centered around the direction of the applied field. The sample is then placed in a solenoid which is in a magnetically shielded area and exposed to a sinusoidally oscillating magnetic field which slowly decreases in amplitude. If the peak value of the oscillating field is B_o, then the moment vector of all particles with coercive fields less than $B_o \cos\theta$, where θ is the angle between the field and the elongated axis, will follow the field as it oscillates. As B_o decreases towards zero, these oscillating particles will gradually be left in one of their two stable states with equal probability, and as a group they will contribute no net moment to the sample. The moment in a sample after this procedure will arise only from unscrambled particles with coercive

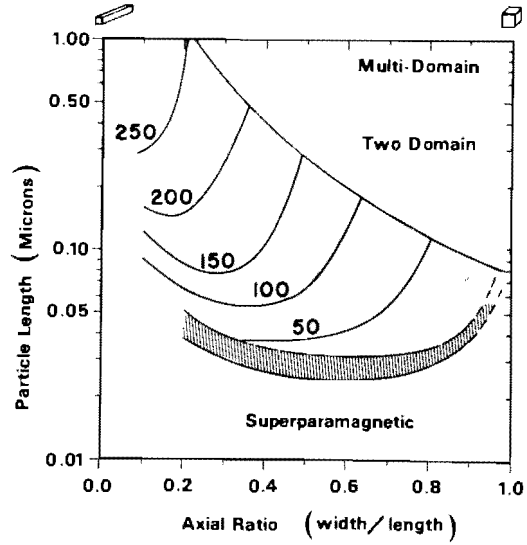

Fig. 14.5.3. Unblocking field for single-domain magnetite grains at 300 K. The horizontal and vertical axes are as on Fig. 14.4.1, with the contours of equal unblocking fields (values in mT) superimposed on the single-domain area. The maximum unblocking field for an elongated magnetite particle is about 300 mT, but most biogenic magnetite crystals fall below 100 mT. (Modified from McElhinny 1973, superimposed on the boundaries of Butler and Banerjee 1975).

fields greater than $B_o \cos\theta$. The $\cos\theta$ term is commonly eliminated from consideration by either tumbling the sample in the coil as the field decreases, or by repeating the procedure separately along three or more axes. The coercivity spectrum can be determined by repeating this procedure and measuring the moment remaining after application of progressively higher peak alternating fields. Examples of this for two mouse tumors are shown in Fig. 14.5.4, and for tissue from the ethmoid area of salmon in Fig. 14.5.5.

A second method for determining the coercivity spectrum is to progressively remagnetize the sample. One starts with a sample that has been completely demagnetized in a strong alternating field as outlined above. It is then progressively remagnetized by exposing it to stronger and stronger fields from an impulse magnetizer or electromagnet, and the remanent moment is measured after each step. An example of this IRM acquisition curve for the ethmoid bones of salmon is shown in Fig. 14.5.5. Although it is extremely easy to make these repetitive acquisition measurements by combining the cotton thread and impulse magnetization techniques discussed earlier, it is not yet possible to correct for the $\cos\theta$ factor as can

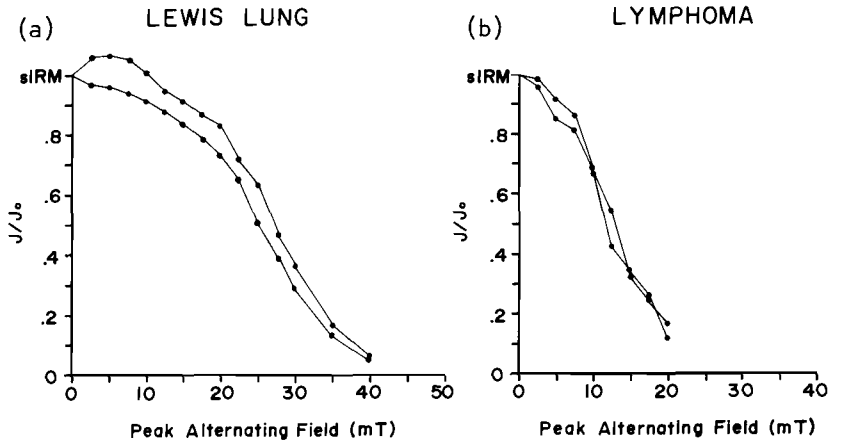

Fig. 14.5.4. Progressive three-axis alternating field demagnetization of two mouse tumors: (a) lewis lung and (b) lymphoma.

be done for Af demagnetization. The net effect, however, is to skew the coercivity distribution towards slightly higher values in exactly the same manner as will Af demagnetization done along only one axis. Because magnetite should not continue to gain additional remanent moment above 0.3 tesla, these IRM acquisition experiments can also be used to identify magnetic contaminants in a sample. Many Fe-Ni alloys used in stainless steel will continue to gain IRM in fields above 1 tesla, and in this way at least one sample of human ethmoid has been found contaminated.

In the ideal case where all of the particles are single domain and dispersed throughout a sample, the one-axis Af demagnetization and IRM acquisition curves should be mirror images of each other. For both, the coercivity spectrum is the absolute value of the derivative of each curve. Cisowski (1981), however, has shown that this is not the case when the single-domain particles are in close proximity to one another, as they are in the chiton teeth (Fig. 14.1.1). Apparently, the strong field of the neighbors of a given particle acting upon it tends to aid the Af demagnetization process, while on the other hand inhibiting the IRM acquisition. Thus, the asymmetry between these techniques can be used to monitor the degree of interparticle interaction, and hence can give some indirect evidence as to the relative grouping of magnetite crystals within a sample.

The example of this shown in Fig. 14.5.5 for salmon is of particular interest. Cisowski found that the shift towards higher coercive fields in the IRM curve was almost exactly matched by the decrease in the Af demagnetization curve. As a result, the ordinate

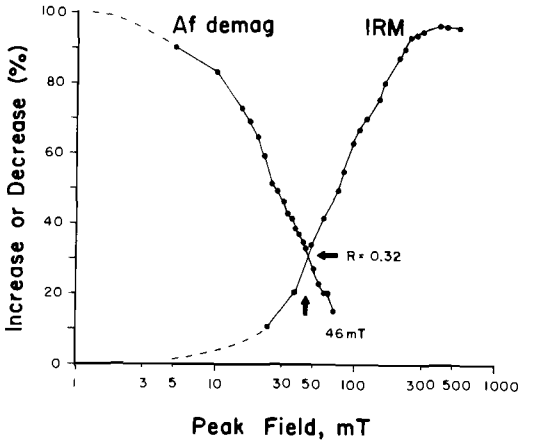

Fig. 14.5.5. Progressive acquisition and Af demagnetization of IRM for salmon ethmoid tissue extracted from four fish. The tissue has greater stability towards Af demagnetization than do most multi-domain magnetite crystals, suggesting that the particles present are single-domain. The flat IRM curve above about 200 mT rules out the presence of the most common laboratory contaminants like hemaetite and metallic iron alloys.

of the intersection point is independent of the interaction effect, and yields the best estimate of the average unblocking field for the particles present. This intersection point for the salmon ethmoid tissue occurs at 46 mT, which corresponds to single-domain magnetite particles which plot just below the 50 mT curve on Fig. 14.5.3. On the other hand, the abscissa of this point is at 32%, well below the 50% level expected for isolated single domains. Cisowski (1981) found that the strongly interacting magnetite crystals in chiton teeth had values of 27%, while a semi-dispersed single-domain powder had a value of 30%. Salmon magnetite crystals are therefore in small isolated clumps or perhaps chains, as are the crystals in the magnetosomes of magnetotactic bacteria. If these are indeed chains, the most probable neuroreceptors involved in magnetoreception would be hair cells, as suggested earlier by Kirschvink and Gould (1981).

It would not be fitting to close this section without at least briefly mentioning three of the other non-destructive weapons developed for the arsenal of rock magnetism, particularly those which have already been or ought to be of eventual use in biomagnetic studies. These include the Lowrie-Fuller test (1971), and its modified anhysteretic version (Dunlop et al. 1973) which are powerful tools for distinguishing multi-domain from single-domain behavior. Similarly, warming a multi-domain magnetite crystal with an un-

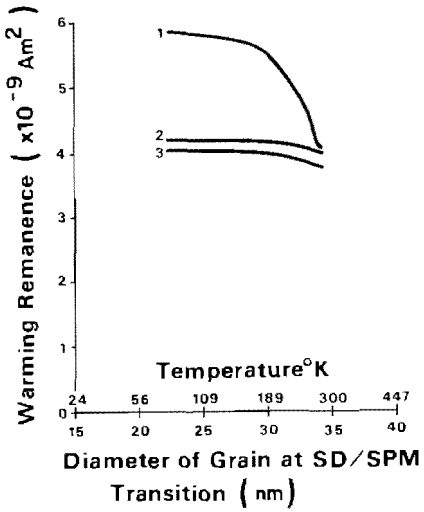

Fig. 14.5.6. Superparamagnetic grains in a worker bee. The temperature at which the remanent moment (remanence) is lost indicates the grain size responsible for that portion of the total moment. The corresponding sizes are shown by the double scale along the bottom. The specimen was first cooled to 77 K in the presence of a strong field (0.3 T). Curve 1 shows the remanent moment of the bee as it warmed in the magnetometer. Curves 2 and 3 show subsequent warming cycles without exposure to the strong magnet.

stable IRM up through magnetite's isotropic point (130 K) can sometimes cause a drop in remanent moment as domain walls realign to a lower energy state; this decrease is also uniquely distinctive for pure magnetite (Ozima et al. 1964) and has already been used to identify magnetite in dolphins (Zoeger et al. 1981). Lastly, detailed information concerning the size distribution of superparamagnetic crystals can be gained by cooling a specimen to 77 K (liquid nitrogen temperature) in the presence of a strong field (0.3 T), forcing all of the moments into alignment, and then continuously monitoring a sample's remanent moment versus temperature as it warms back to room temperature (≈300 K). As the individual crystals warm through their single-domain/superparamagnetic transition, they will lose their stable remanent moment and the total moment will drop accordingly. This experiment for the honey bee (Fig. 14.5.6) shows that most of the moment is lost as the superparamagnetic transition goes from 30 to 35 nm. A magnetite sphere 32.5 nm in diameter has a moment of about 8.6×10^{-16} A·m^2, so about 2×10^8 of them are necessary to account for the lost signal. This suggests

that they have at least this number of such particles, most of which fall in the size region between 30-35 nm. The biological function of these particles, if any, is as yet unknown.

14.5.8. Extraction and Characterization of Biogenic Magnetite

Although the indirect magnetic techniques discussed above are good for characterizing the bulk ferromagnetic properties of a sample, it is eventually necessary to extract the magnetic particles from the host tissue, purify and identify them, and examine the resulting material with the scanning or transmission electron microscope. Initial attempts to extract the particles using purified 5% Na-hypochlorite digestion were not very successful (Kirschvink 1981b), probably because the fine particles were sticking to something. A simple solution to this problem which has recently been found (M.M. Walker, pers. comm.) is to first extract the soluble lipids by using ether, and then digest the remaining tissue with hypochlorite. Magnetic particles can then be separated from the solution by holding a small hand magnet adjacent to the glass digesting tube. A variety of techniques can in principal be used at this stage for identifying the purified material, including x-ray diffraction (Lowenstam 1962), Mössbauer absorption (Frankel et al. 1979), Curie temperature analysis (Gould et al. 1978), or electron diffraction on the transmission electron microscope (Towe and Moench 1981). Electron diffraction requires the least amount of material, and under favorable circumstances can identify single submicron crystals. If tens or hundreds of such particles are present, the more easily obtained spot patterns like that shown in Fig. 14.1.3 are equally distinctive.

ACKNOWLEDGEMENTS

I greatly thank H. Lowenstam, K.M. Towe, M.M. Walker, A.J. Perry, A. Dizon, and K. Peterson for helpful discussions and use of their scanning and transmission electron micrographs. Contribution 3810 from the Division of Geological and Planetary Sciences of the California Institute of Technology. Various phases of this work were supported by NSF Grants SPI79-14845, BNS78-24754, PCM82-03627, EAR78-03204, EAR81-21377, and the Prince Charitable Trusts.

Partial list of references:

Balkwill, D. L., D. Maratea, et al. (1980). "Ultrastructure of a magnetotactic spirillum. ." J. Bacteriol. **141**(3): 1399-1408.

Blakemore, R. (1975). "Magnetotactic bacteria." Science **190**: 377-379.

Blakemore, R., R. Frankel, et al. (1980). "South-seeking magnetotactic bacteria in the southern hemisphere." Nature **286**: 384-385.

Blakemore, R., D. Mareta, et al. (1979). "Isolation and pure culture of a freshwater magnetic spirillum in chemically defined medium." J. Bacteriol. **140**: 720-729.

Butler, R. F. and S. K. Banerjee (1975). "Theoretical single-domain size range in magnetite and titanomagnetite." J. Geophys. Res. **80**: 4049-4058.

Cisowski, S. (1981). "Interacting vs. non-interacting single-domain behavior in natural and synthetic samples." Phys. Earth Planet. Inter. **26**: 56-62.

Demitrack, A. (1981). "A search for bacterial magnetite in the sediments of a freshwater marsh." EOS, Transactions-American Geophysical Union **62**: 850.

Denham, C., R. Blakemore, et al. (1980). "Bulk Magnetic Properties of Magnetotactic Bacteria." IEEE Transactions on Magnetics **MAG-16**(5).

Frankel, R. B. and R. P. Blakemore (1980). "Navigational compass in magnetic bacteria." J. Magn. Magn. Mater. **15-18**: 1562-1564.

Frankel, R. B., R. P. Blakemore, et al. (1981). "Magnetotactic bacteria at the geomagnetic equator." Science **212**: 1269-1270.

Frankel, R. B., R. P. Blakemore, et al. (1979). "Magnetite in freshwater magnetotactic bacteria." Science **203**: 1355-1356.

Goree, W. S. and M. Fuller (1976). "Magnetometers using Rf-driven SQUIDS and their applications in rock magnetism and paleomagnetism." Rev. Geophys. Space Phys. **14**: 591-608.

Gould, J. L. (1980). "The case for magnetic sensitivity in birds and bees (such as it is." American Scientist **68**: 256-267.

Gould, J. L., J. L. Kirschvink, et al. (1978). "Bees have magnetic remanence." Science **201**: 1026-1028.

Jones, D. S. and B. J. MacFadden (1982). "Induced magnetization in the monarch butterfly, Danaus plexippus (Insecta, Lepidoptera)." J. Exp. Biol. **96**: 1-9.

Jungerman, R. L. and B. Rosenblum (1980). "Magnetic induction for the sensing of magnetic fields by animals - an analysis." J. Theor. Biol. **87**: 25-32.

Kalmijn, A. J. (1974). The detection of electric fields from inanimate and animate sources other than electric organs. Handbook of Sensory Physiology. A. Fessard. **9:** 147-200.

Kalmijn, A. J. and R. P. Blakemore (1978). The magnetic behavior of mud bacteria. Animal Migration, Navigation and Homing , . K. Schmidt-Koenig and W. T. Keeton. Berlin, Springer-Verlag**:** 354-355.

Keeton, W. T. (1971). "Magnets interfere with pigeon homing." Procd. Natl. Acad. Sci. USA **68**: 102-106.

Kirschvink, J. L. (1980). "South-seeking magnetic bacteria." Journal of Experimental Biology **86**: 345-347.

Kirschvink, J. L. (1981). "The horizontal magnetic dance of the honey bee is compatible with a single-domain ferromagnetic magnetoreceptor,." Bio Systems **14,**: 193-203.
Kirschvink, J. L. (1982). "Birds, bees and magnetism: A new look at the old problem of magnetoreception (review article),." Trends in Neurosciences **5**: 160-167.
Kirschvink, J. L. and J. L. Gould (1981). "Biogenic magnetite as a basis for magnetic field sensitivity in animals,." Bio Systems **13**: 181-201.
Kirschvink, J. L. and H. A. Lowenstam (1979). "Mineralization and magnetization of chiton teeth: Paleomagnetic, sedimentologic, and biologic implications of organic magnetite." Earth & Planetary Science Letters **44**: 193-204.
Kittel, C. (1976). Introduction to Solid State Physics, 5th edition. New York, John Wiley & Sons.
Lazaroff, N., W. Sigal, et al. (1982). "Iron Oxidation and Precipitation of Ferric Hydroxysulfates by Resting Thiobacillus ferrooxidans Cells." Applied and Environmental Microbiology **43**(4): 924-938.
Lins de Barros, H. G. P., D. M. S. Esquivel, et al. (1981). "Magnetotactic algae." Acad. Bras. Cienc. Notas Fis. **CBPF-NF**(048/81).
Lowenstam , H. A. (1962). "Magnetite in denticle capping in recent chitons (*polyplacophora*)." Geol. Soc. Am. Bull. **73**: 435-438.
Lowenstam, H. A. (1981). "Minerals made by organsims." Science **211**: 1126-1131.
Lowenstam, H. A. and S. Weiner (1982). Mineralization by organisms and the evolution of biomineralization. Biomineralization and Biological Metal Accumulation: Biological and Geological Perspective. Papers presented at the Fourth International Symposium on Biomineralization. P. Westbroek and E. W. DeJong, Kreidel Press.
Lowrie, W. and M. Fuller (1971). "On the alternating-field demagnetization characteristics of multidomain thermoremanent magnetization in magnetite." J. Geophys. Res. **76**: 6339-6349.
Martin, H. and M. Lindauer (1977). "Der Einfluss der Erdmagnetfelds und die Schwerorientierung der Honigbiene." J. Comp. Physiol. **122**: 145-187.
Mather, J. G. and R. R. Baker (1981). "Magnetic sense of direction in woodmice for route-based navigation." Nature **291**: 152-155.
McElhinny, M. W. (1973). Paleomagnetism and Plate Tectonics. Cambridge, U.K., Cambridge University Press.
Ossenkopp, K. P. and R. Barbeito (1978). "Bird orientation and the geomagnetic field: a review." Neuroscience and Biobehavioral Review **2**: 255-270.
Phillips, J. B. and K. Adler (1978). Directional and discriminatory responses of salamanders to weak magnetic fields. In: . Animal Migration, Navigation, and Homing. K. Schmidt-Koenig and W. T. Keeton. Berlin, Springer-Verlag**:** 325-333.
Quinn, T. P. (1980). "Evidence for celestial and magnetic compass orientation in lake migrating sockeye salmon fry." J. Comp. Physiol. A **137**: 243-248.
Tesch, F.-W. (1980). Migratory performance and environmental evidence of orientation. Environmental Physiology of Fishes. M. A. Ail. Ney York, Plenum Press**:** 589-612.

Towe, K. and T. Moench (1981). "Electron-Optical Characterization of Bacterial Magnetite " Earth and Planetary Science Letters **52** 213-220.
Towe, K. M. and H. A. Lowenstam (1967). "Ultrastructure and development of iron mineralization in the radular teeth of Cryptochiton stelleri (Mollusca)." Journal of Ultrastructural Research **17**: 1-13.
Walcott, C. (1980). "Homing pigeon vanishing bearings at magnetic anomalies are not altered by bar magnets." J. Exp. Biol. **86**: 349-352.
Walcott, C., J. L. Gould, et al. (1979). "Pigeons have magnets." Science **205**: 1027-1029.
Walcott, C. and R. P. Green (1974). "Orientation of homing pigeons altered by a change in the direction of an applied magnetic field." Science **184**: 180-182.
Walker, M. M. and A. E. Dizon (1981). "Identification of magnetite in tuna." EOS, Transactions-American Geophysical Union **62**: 850.
Wiltschko, W. and R. Wiltschko (1972). "Magnetic compasses of European robins." Science **176**: 62-64.
Yeagley, H. L. (1947). "A preliminary study of a physical basis of bird navigation." J. Appl. Phys. **18**: 1035-1063.
Yorke, E. D. (1979). "A possible magnetic transducer in birds." J. Theor. Biol. **77**: 101-105.
Yorke, E. D. (1981). "Sensitivity of pigeons to small magnetic field variations." J. Theor. Biol. **89**: 533-537.
Zoeger, J., J. R. Dunn, et al. (1981). "Magnetic material in the head of a common Pacific dolphin." Science **213**: 892-894.

NATO Advanced Science Institutes Series

A series of edited volumes comprising multifaceted studies of contemporary scientific issues by some of the best scientific minds in the world, assembled in cooperation with NATO Scientific Affairs Division.

This series is published by an international board of publishers in conjunction with NATO Scientific Affairs Division

A Life Sciences **B Physics**	Plenum Publishing Corporation New York and London
C Mathematical and Physical Sciences	D. Reidel Publishing Company Dordrecht, Boston, and London
D Behavioral and Social Sciences **E Applied Sciences**	Martinus Nijhoff Publishers The Hague, Boston, and London
F Computer and Systems Sciences **G Ecological Sciences**	Springer Verlag Heidelberg, Berlin, and New York

Recent Volumes in Series A: Life Sciences

Volume 60—The Use of Human Cells for the Evaluation of Risk from Physical and Chemical Agents
edited by Amleto Castellani

Volume 61—Genetic Engineering in Eukaryotes
edited by Paul F. Lurquin and Andris Kleinhofs

Volume 62—Heart Perfusion, Energetics, and Ischemia
edited by Leopold Dintenfass, Desmond G. Julian, and Geoffrey V. F. Seaman

Volume 63—Structure and Function of Plant Genomes
edited by Orio Ciferri and Leon Dure III

Volume 64—Gene Expression in Normal and Transformed Cells
edited by J. E. Celis and R. Bravo

Volume 65—The Pineal Gland and Its Endocrine Role
edited by J. Axelrod, F. Fraschini, and G. P. Velo

Volume 66—Biomagnetism: An Interdisciplinary Approach
edited by Samuel J. Williamson, Gian-Luca Romani, Lloyd Kaufman, and Ivo Modena

Biomagnetism

An Interdisciplinary Approach

Edited by

Samuel J. Williamson

New York University
New York, New York

Gian-Luca Romani

Istituto di Elettronica dello Stato Solido—C N R
Rome, Italy

Lloyd Kaufman

New York University
New York, New York

and

Ivo Modena

Seconda Università di Roma and
Istituto di Elettronica dello Stato Solido—C N R

Plenum Press
New York and London
Published in cooperation with NATO Scientific Affairs Division